AGU PUBLICATIONS

Geochemistry, Geophysics, Geosystems

RESEARCH ARTICLE

10.1002/2013GC005087

Key Points:

- Strain data analysis from explosions/degassing events at Soufriere Hills Volcano
- Pressure release deep within the magmatic system sec-min prior to events
- Rapid gas rise from magma reservoir to surface via tensile hydraulic fractures

Correspondence to:
S. Hautmann,
stefanie.hautmann@googlemail.com

Citation:
Hautmann, S., F. Witham, T. Christopher, P. Cole, A. T. Linde, I. S. Sacks, and S. J. Sparks (2014), Strain field analysis on Montserrat (W.I.) as tool for assessing permeable flow paths in the magmatic system of Soufrière Hills Volcano, *Geochem. Geophys. Geosyst.*, *15*, 676–690, doi:10.1002/2013GC005087.

Received 8 OCT 2013
Accepted 29 JAN 2014
Accepted article online 5 FEB 2014
Published online 21 MAR 2014

Strain field analysis on Montserrat (W.I.) as tool for assessing permeable flow paths in the magmatic system of Soufrière Hills Volcano

Stefanie Hautmann[1], Fred Witham[1,2], Thomas Christopher[3], Paul Cole[3,4], Alan T. Linde[5], I. Selwyn Sacks[5], and R. Stephen J. Sparks[1]

[1]School of Earth Sciences, University of Bristol, Bristol, UK, [2]Now at Rolls-Royce, Bristol, UK, [3]Montserrat Volcano Observatory, Flemmings, Montserrat, British West Indies, [4]Now at School of Geography, Earth and Environmental Sciences, Plymouth University, Plymouth, UK, [5]Department of Terrestrial Magnetism, Carnegie Institution of Washington, Washington, District of Columbia, USA

Abstract Strain dilatometers have been operated on the volcanic island of Montserrat (West Indies) for more than a decade and have proven to be a powerful technique to approach short-term dynamics in the deformational field in response to pressure changes in the magmatic system of the andesitic dome-building Soufrière Hills Volcano (SHV). We here demonstrate that magmatic activity in each of the different segments of the SHV magmatic system (shallow dyke-conduit, upper and lower magma chambers) generates a characteristic strain pattern that allows the identification of operating sources in the plumbing system based on a simple scheme of amplitude ratios. We use this method to evaluate strain data from selected Vulcanian explosions and gas emission events that occurred at SHV between 2003 and 2012. Our results show that the events were initiated by a short phase of contraction of either one or both magma chambers and a simultaneous inflation of the shallow feeder system. The initial phase of the events usually lasted only tens to hundreds of seconds before the explosion/gas emission started and the system recovered. The short duration of this process points at rapid transport of fluids rather than magma ascent to generate the pressure changes. We suggest the propagation of tensile hydraulic fractures as viable mechanism to provide a pathway for fluid migration in the magmatic system at the observed time scale. Fluid mobilization was initiated by a sudden destabilization of large pockets of already segregated fluid in the magma chambers. Our study demonstrates that geodetic observables can provide unprecedented insights into complex dynamic processes within a magmatic system commonly assessed by theoretical modeling and petrologic observations.

1. Introduction

Soufrière Hills Volcano (SHV), Montserrat, West Indies, has been in a heightened state of activity since 1995, with periodically repeating episodes of lava dome extrusion and discrete short-lived events, such as dome collapses, Vulcanian explosions, gas emission, and ash venting events [*Wadge et al.*, 2014]. Variations in the deformational field in response to changes in eruption dynamics of the active SHV are continuously monitored by a network of cGNSS (continuous Global Navigation Satellite System) antennas/receivers and Sacks-Evertson borehole dilatometers. While long-term changes in ground deformation are usually assessed via cGNSS data [e.g., *Elsworth et al.*, 2008; *Hautmann et al.*, 2010], the satellite-based measurements have proven unsuitable for the detection of short-term events [*Hautmann et al.*, 2013]. Thus, the network of strainmeters complements satellite-based geodetic monitoring techniques (e.g., InSAR, cGNSS), as it offers the opportunity to resolve deformational signals at short time scales.

The analysis and modeling of strain data collected since 2003 has revealed that specific short-lived events in volcanic activity, such as a dome collapse [*Voight et al.*, 2006], Vulcanian explosions [e.g., *Linde et al.*, 2010; *Chardot et al.*, 2010] and short-term lava extrusion phases [*Hautmann et al.*, 2013], generate signals with characteristic fingerprints in the strain records. Strain field analysis offers a simple approach to relate eruptive events at SHV to associated pressure evolution within the magmatic system [e.g., *Voight et al.*, 2006; *Linde et al.*, 2010; *Hautmann et al.*, 2013]. Based on earlier studies, we present an overview of the characteristic pattern of strain changes on Montserrat and will highlight how strain data enable the determination of operating sources in the SHV magmatic system during a particular eruption event.

Amongst the most common and frequently observed short-term eruptive events at SHV are Vulcanian eruptions, which are mostly unheralded, discrete, and violent explosions that last on the order of seconds to minutes. The events are characterized by atmospheric shock waves, the eruption of pyroclastic rocks, which include tephra, ballistic bombs and blocks along with ash plumes that usually rise to altitudes of atmospheric heights of several kilometers [e.g., *Formenti et al*., 2003]. Other short-lived volcanic events include intense gas emission (up to 10 times above average) commonly associated with intermittent vigorous ash-venting, typically lasting a few hours to no longer than a few days. This type of event is not classified as a Vulcanian eruption, as it is of nonexplosive nature. Between 2003 and 2012, several Vulcanian explosions and gas emission events have been captured by strain records from SHV. The analysis of continuous strain records allows not only for the identification of operating segments in the magmatic system during an eruptive event, but additionally gives precise constraints on the time scale during which pressure changes occur. The gathered data, therefore, provides unprecedented and unique insights into the driving mechanisms of the observed explosions and gas emission events.

The purpose of the following paper is twofold. First, we summarize the results from strain data analysis reported in a number of studies that have been conducted since the beginning of strainmeter installation on Montserrat in order to give an overview of the interpretation and application of strain data in terms of discerning the operating sources in the magmatic system of SHV. Second, we focus on a series of Vulcanian explosions and gas emission events, which were documented in strain records between 2003 and 2012. Decompression of magma chambers together with pressure increases within the shallow dyke-conduit plumbing system over time scales of seconds to minutes give for the first time evidence for rapid fluid migration throughout the magmatic system of SHV. We augment our strain data with corecorded volcano monitoring data in order to evaluate underlying dynamic processes.

2. Magmatic System of Soufrière Hills Volcano

Combining the results of numerous studies that focus on the analysis and modeling of mostly geodetic (GNSS, strain, and tilt), but also seismic and petrologic data, gives some constraints on the subsurface plumbing system of SHV (simplified scheme shown in Figure 1). Gas emission, petrologic, GPS and strain data, seismic tomography, and thermal modeling [*Murphy et al*., 2000; *Edmonds et al*., 2001; *Annen et al*., 2006, 2014; *Elsworth et al*., 2008; *Paulatto et al*., 2012] suggest that the magmatic system of SHV consists of two vertically stacked magma chambers. A vertically prolate lower magma chamber (LMC) that is centered at about 12.5 km below sea level [*Hautmann et al*., 2010] and an approximately spherical upper magma chamber (UMC) that is centered at about 5.5 km b.s.l. [*Aspinall et al*., 1998; *Barclay et al*., 1998; *Devine et al*., 1998; *Mattioli et al*., 1998; *Voight et al*., 2006; *Wadge et al*., 2006; *Paulatto et al*., 2012] is one model. Geophysical data indicate that both chambers are directly connected [*Elsworth et al*., 2008]. Although this connection is commonly depicted as a conduit, the nature of it has not been resolved, since this segment of the magmatic system is invisible to geodetic data recorded at the surface [*Hautmann et al*., 2010] and tomographic images are not resolved below 8 km [*Paulatto et al*., 2012]. The volume ratio UMC:LMC has been constrained by strain data analyses to 1:3, with 8 km^3 as minimum volume estimation for the UMC [*Hautmann et al*., 2013]. Similar chamber volumes were independently inferred from studies that integrate seismic tomography with thermal models [*Paulatto et al*., 2012] and models of nonlinear fluid-flow in a dual chamber-conduit systems [*Melnik and Costa*, 2014]. Based on thermodynamic models on eruption activity, the UMC was suggested to be coupled to a dyke-conduit plumbing system at shallow depths that feeds the eruption at the surface [*Costa et al*., 2007]. The dyke-conduit structure inferred for the shallow plumbing system was confirmed by geodetic data analysis. The dyke was constrained to be oriented in NW-SE direction with a lateral extension between 0.5 and 1 km [e.g., *Mattioli et al*., 1998; *Hautmann et al*., 2009; *Linde et al*., 2010; *Hautmann et al*., 2013]. At approximately 1–1.5 km below the vent the dyke is thought to blend into a cylindrical conduit that measures about 15 m radius at the surface [*Costa et al*., 2007]. Note that in our study we invoke only the physical feature of the dyke-conduit geometry of the shallow plumbing system, but not the process of nonlinear magma flow within the dyke that was inferred by *Costa et al*. [2007] for cyclic eruption activity.

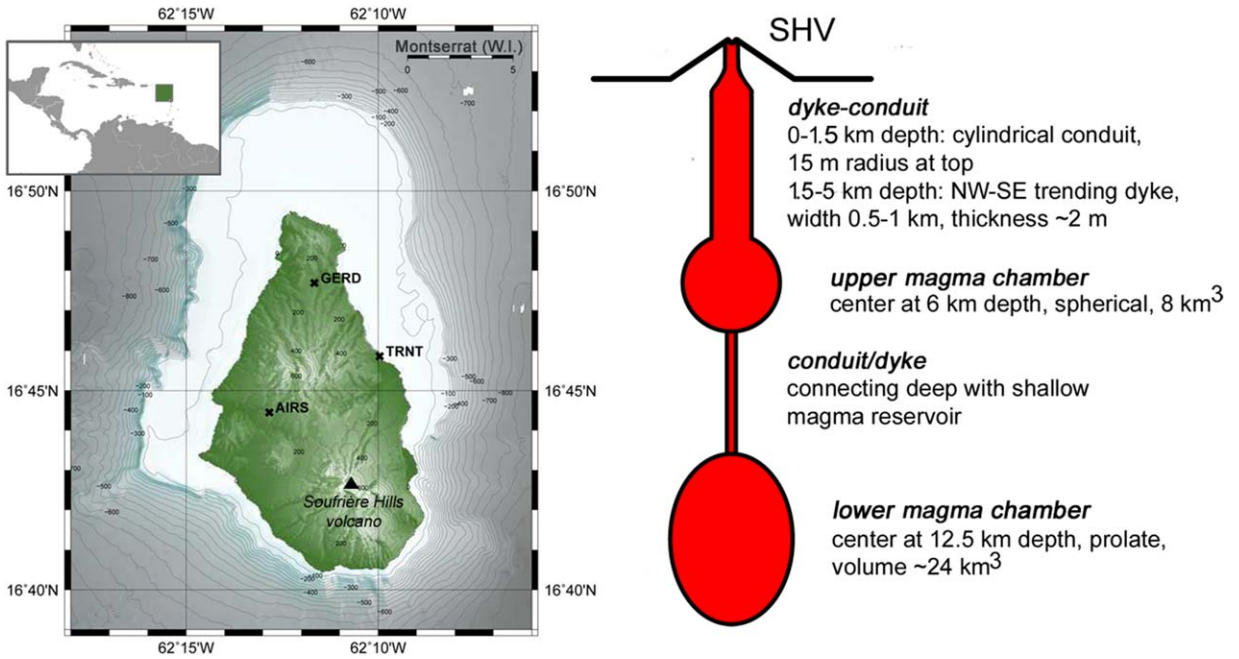

Figure 1. (left) Topographic map of Montserrat showing the location of the active Soufrière Hills Volcano (SHV) and the sites of strainmeter installations (black cross). Inlay map gives the location of Montserrat in the Lesser Antilles. (right) Model of the active magmatic system of SHV as inferred from earlier studies. See text for details.

3. Strain Data from Montserrat

Three Sacks-Evertson borehole strainmeters are installed on Montserrat at a depth of 200 m below the surface. The site most distant from the volcano (GERD) is positioned 9.6 km NNW of the active vent. The two more proximate sites are located just at the entrance to the volcano hazard ("exclusion") zone 5.2 km NW (AIRS) and 6.9 km NNE (TRNT) of the volcano (Figure 1). The near sites subtend an angle of 65°, with AIRS being located along the most likely strike direction of the shallow feeder dyke. All instruments were calibrated in situ to an absolute level via earth strain tides, while long period (~80 s) surface waves from distant teleseismic events were used to accurately determine the relative sensitivities of the sites.

The strain field at the surface is characterized by a nodal line, marking the reversal of the sign of volumetric strain changes. The trace of the nodal line depends on the depth and the geometry of the magmatic body generating the signal, while the source volume and/or pressure changes within the source affect only the magnitude of strain, but not the location of the nodal line and the relative signal ratios between the individual sites. Hence, in contrast to other geodetic techniques (such as GNSS, tilt, and gravity), strain measurements have the important advantage of permitting the constraint of source parameters with data from three instruments only, given that the three instruments are positioned in a suitable array in relation to the pressure source. This requirement is met on Montserrat as the combination of the spatial distribution of strainmeters on island and the structure of the active SHV magmatic system enables us to reveal and quantify the contribution of each individual segment of the plumbing system to a recorded strain signal. The following section gives details on the characteristics of the different strain pattern that relate to pressure changes in each of the individual segments of the magmatic system.

3.1. Strain Variations Due to Individual Storage Components

Pressure changes in the uppermost conduit were documented in strain records during a series of Vulcanian explosions that took place on 13–15 July 2003 [*Voight et al.*, 2010], on 29 July 2008 [*Gottsmann et al.*, 2011] and on 3 January 2009 [*Chardot et al.*, 2010]. Recorded data from the explosions give ratios of the strain signal of AIRS/TRNT = 2 and of AIRS/GERD = 4. Model predictions on strain changes in response to inflation/deflation of the uppermost conduit fit the observations (AIRS/TRNT = 1.9 and AIRS/GERD = 4.3; see Table 1 for comparison of observed versus model predicted strain ratios) and constrain the nodal line at a distance

Table 1. Observed and Modelled Strain Amplitude Ratios.

Operating Segment in magmatic system[a]	Strain Amplitude Ratios					
	Observed			Modeled		
	AIRS/TRNT	AIRS/GERD	TRNT/GERD	AIRS/TRNT	AIRS/GERD	TRNT/GERD
Conduit[b]	2.0	4.0	2.0	1.9	4.3	2.3
Dyke				−1.4	−18.0	13.0
UMC[c]	1.2	−1.9	−1.6	2.5	−4.2	−1.7
LMC				1.2	2.0	1.7
UMC + dyke	−0.8	−3.8	4.8	−0.8	−4.2	5.6
LMC + UMC + dyke	0.8	5.1	6.4	0.8	5.1	6.4

[a]UMC = upper magma chamber, LMC = lower magma chamber.
[b]Strain changes of order a few nanostrains (ns) only.
[c]Recorded data distorted by loading effects from associated dome collapse.

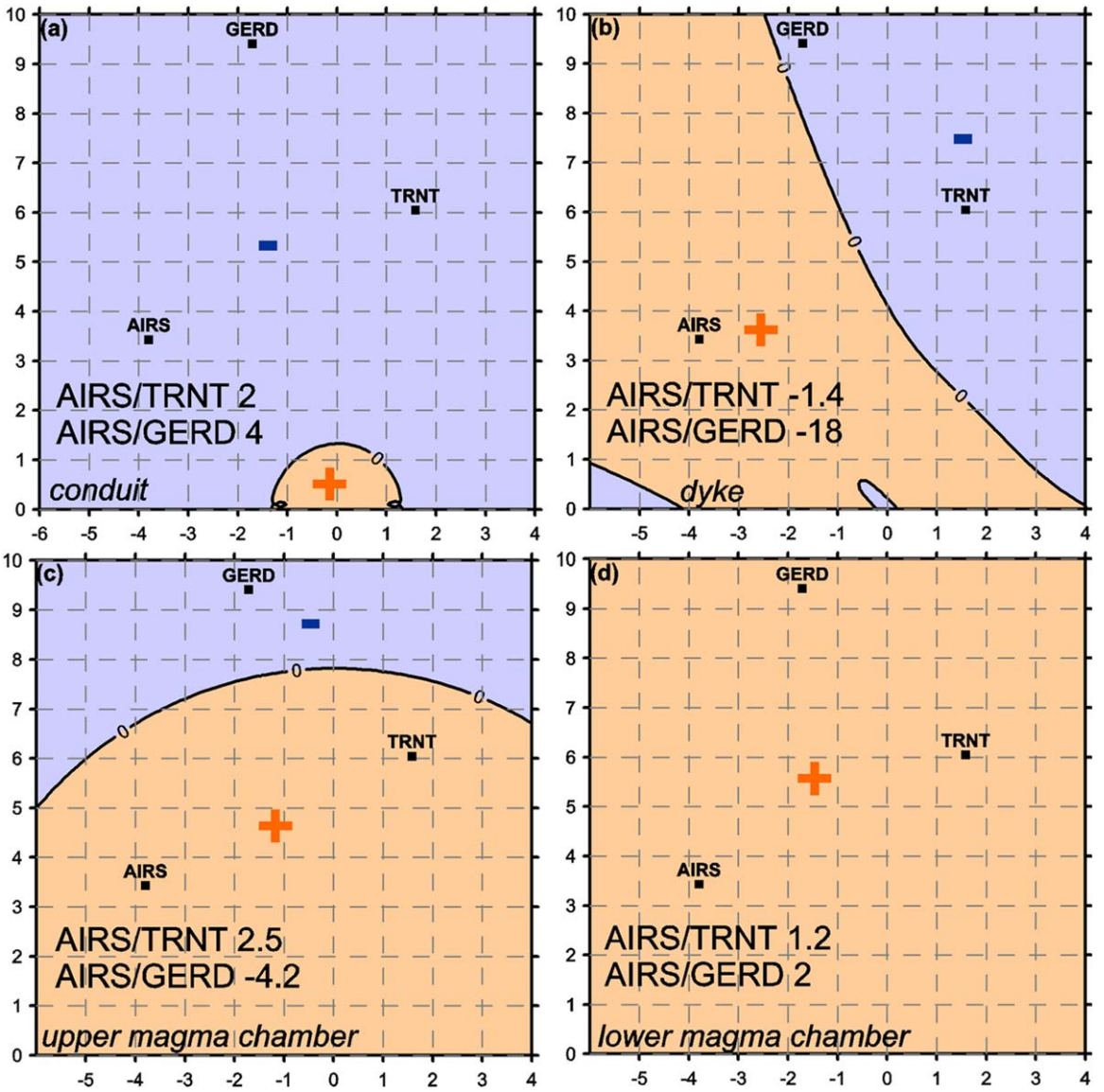

Figure 2. Resulting surface strain pattern due to inflation of either (a) the conduit, (b) the dyke, (c) the upper magma chamber, or (d) the lower magma chamber. The plots indicate the run of the nodal line, which marks the signal reversal in volumetric strain changes. Positive strain (shaded in orange) indicates volumetric expansion, while negative strain (shaded in blue) indicates contraction. Pressure changes in each of the segments of the magmatic system generate strain changes at the sampling sites AIRS, GERD, and TRNT at a specific ratio. As such, strain ratios are indicative for the determination of operating sources during an eruption event. Note that the magnitude of pressure changes only influences the absolute strain changes, but not the relative ratios.

of 1.4 km radially around the active vent [*Chardot et al*., 2010]. Hence, strain changes resulting from pressure variations within the uppermost conduit are of same signal polarity at all sites (Figure 2a). However, observations show that, due to the small volume of the conduit, the maximum amplitude of recorded strain changes is of order a few nanostrains (ns) only. For this reason, the effect of the conduit signal cannot be separated if other segments in the magmatic system are additionally involved, as the dyke and magma chamber signals swamp the conduit signal. The possible contribution of the conduit signal can, therefore, be neglected in the analysis of data that additionally include activity in the deeper magmatic system.

The NW-SE oriented feeder dyke is the only known segment in the SHV magmatic system with a vertically bilateral geometry. Hence, unlike the strain signals generated by all other magma bodies in the magmatic system, the nodal line in the strain field that results from dilation/deflation of the dyke is not radially symmetrical around the vent, but follows a NW-SE trend, similar to the dyke orientation (Figure 2b). Therefore, eruptive activity that involves pressure changes in the dyke can be easily identified in the strain records due to a switch in signal polarity along a NW-SE line, hence, between AIRS and TRNT. Lacking direct observations on pressure changes exclusively within the shallow dyke, expected strain ratios have been constrained via analytical models. Inferred signal ratios are AIRS/TRNT $= -1.4$ and AIRS/GERD $= -18$ [*Linde et al*., 2010; *Hautmann et al*., 2013].

Pressure changes in just the UMC result in a nodal line of the strain signal that runs concentrically around the vent between the distant site GERD and the near sites AIRS and TRNT, as it was first recognized in data from the major dome collapse on 3 July 2003 [*Voight et al*., 2006]. The strain data revealed a postcollapse expansion of a slightly oblate UMC due to pressure release at the surface. The amplitude ratios documented for this event are AIRS/TRNT $= 1.2$ and AIRS/GERD $= -1.9$, however, the records were significantly influenced by additional effects such as ash fall, the removal of the dome and offshore deposition of the collapsed mass [*Voight et al*., 2006]. The magnitudes of the strain signals associated to these additional factors are difficult to assess though and strain analysis from later events (March 2004 Vulcanian explosion) [*Linde et al*., 2010] revealed somewhat larger ratios AIRS/TRNT $= 2.5$ and AIRS/GERD $= -4.2$, which translates to a spherical rather than an oblate geometry of the UMC, an inference also supported by seismic tomography [*Paulatto et al*., 2012] and analysis of GPS data from the early stage of the eruption [*Mattioli et al*., 1998]. It seems likely that the data related to the dome collapse are distorted by loading effects and that the amplitude ratios are actually larger than inferred from this particular event in July 2003. Despite the uncertainties in the strain ratio AIRS/GERD—the switch in signal polarity between the near sites and the far site is a distinctive characteristic of the strain pattern resulting from pressure changes in just the UMC (Figure 2c).

Finally, decompression/compression of solely the LMC has only been documented in cGNSS data of 2–3 year episodes of ground inflation/deflation between 2003 and 2007 [*Elsworth et al*., 2008; *Hautmann et al*., 2010]. Due to a unconstrained long-term drift of the strainmeters and occasionally required restarts of the strain installations (after e.g., flooding, lightning, anthropogenic damage at the sites), time series strain records from periods longer than several weeks are unsuitable for data analysis. The strain pattern resulting from LMC expansion/contraction has, therefore, been constrained from theoretical forward modeling. The models predict the nodal line to be positioned far beyond the distant site GERD (Figure 2d), resulting in identical signal polarities at all operating strain sites with ratios of AIRS/TRNT $= 1.2$ and of AIRS/GERD $= 2$.

3.2. Strain Variations Due to Multiple Storage Components

Some eruptive events have been found to be driven by more than just one segment of the magmatic system. During events in which the individual segments act together as an open system, the pressure changes are similar in each segment of the plumbing system [*Linde et al*., 2010; *Hautmann et al*., 2013]. For this reason, even though the absolute magnitude of the signal might change in different events, the relative signal ratios between the individual sites is constant for the presented scenarios.

The strain signal associated with the Vulcanian explosion on 3 March 2004 was found to be generated by a decompression of the UMC combined with a dilation of the dyke [*Linde et al*., 2010]. The observed strain pattern shows a signal reversal between AIRS (expansion) versus TRNT and GERD (contraction) with a ratio AIRS/TRNT $= -0.8$ and a ratio AIRS/GERD $= -3.8$ (Figure 3a). Model predicted strain ratios for combined

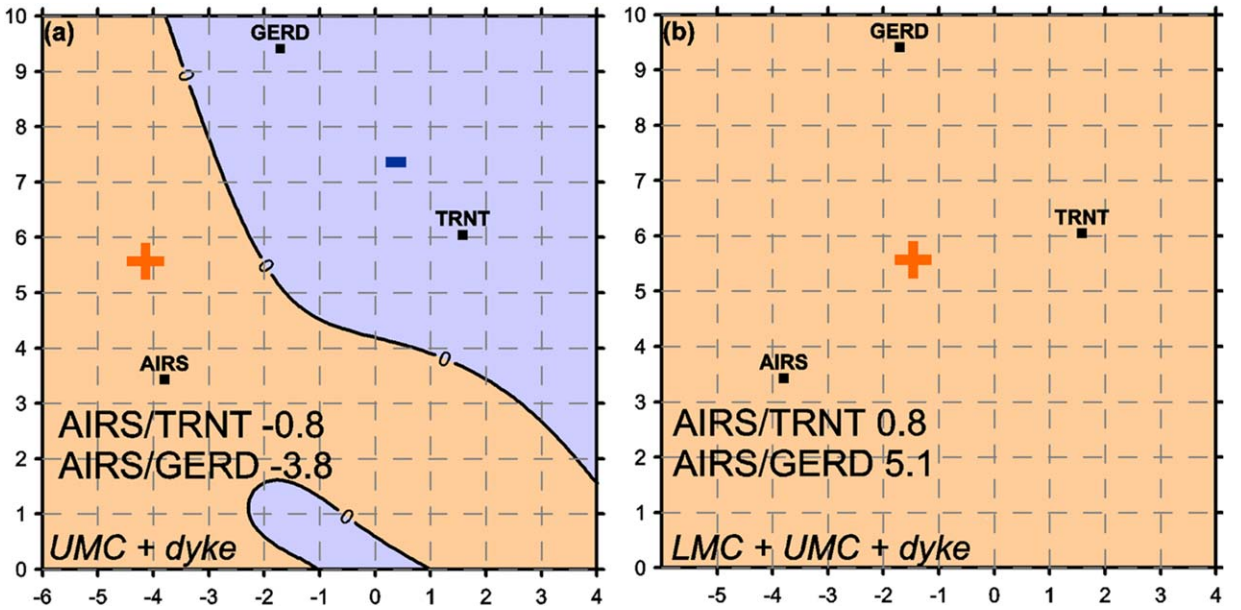

Figure 3. (a) Strain pattern at the surface due to deflation of the upper magma chamber (UMC) together with an inflation of the shallow feeder system (observed during a Vulcanian explosion in March 2004) [*Linde et al*., 2010]. (b) Strain pattern at the surface due to deflation of lower and upper magma chamber (LMC + UMC) together with an inflation of the shallow feeder system (observed during a lava extrusion event in December 2008/January 2009) [*Hautmann et al*., 2013]. Positive strain (shaded in orange) indicates volumetric expansion, while negative strain (shaded in blue) indicates contraction.

UMC and dyke activity were found to be similar with AIRS/TRNT = −0.8 and AIRS/GERD = −4.2 [*Linde et al*., 2010].

A 4 weeks episode of increased lava dome extrusion took place from 8 December 2008 to 3 January 2009. Corecorded strain data revealed that the event was driven by the entire magmatic system, in particular, by a decompression of both magma chambers along with a simultaneous dilation of the dyke [*Hautmann et al*., 2013]. The inferred pressure variations were interpreted as the ascent of magma out of the two chambers into the dyke and partly further up to the surface. For this scenario the signal polarity is the same for all sites (contraction), with observed and modeled signal ratios of AIRS/TRNT = 0.8 and AIRS/GERD = 5.1 (Figure 3b).

3.3. Applicability and Limitation of Strain Data for Interpretation of Activity Events at SHV

We have summarize how the ratio and the polarity of the strain signals recorded along the network of dilatometers on Montserrat give an unequivocal estimate of the sources operating in the magmatic system of SHV. We thus can infer a simple scheme that uses the amplitude ratios of strain to facilitate the identification of operating sources in the magmatic system (Table 1). As such, based on the inferred structure of the magmatic system, strain data from Montserrat offer a unique opportunity to evaluate the dynamics in the volcanic system during or immediately after short-term volcanic events. A limitation to this approach is that one cannot exclude the existence of any additional sources in the magmatic system that so far might not have been detected or considered to contribute to geodetic signals recorded on Montserrat. For example, we cannot exclude a contribution from the magma pathway connecting the two chambers. Minor uncertainties in source characteristic estimations (e.g., ±0.5 km variation in magma chamber depth) affect the resulting strain field only slightly. Thus magma bodies entirely different in geometry and/or depth from the sources described above, would generate a signal with entirely different strain polarities/ratios. Therefore, the observation of a new pattern of strain polarities/ratios would be an immediate indicator for unknown and unconstrained dynamic processes in the active magmatic system.

A new study conducted by *Pascal et al*. [2012] investigated the misfit that results from disregarding the effect of source interaction on surface deformation when combining Mogi and Okada analytical sources. A case study adapted to Montserrat showed that significant discrepancies arise only for near-field vertical deformation (<2 km from the vent) in response to pressurization of the superimposed magma chambers.

Due to the network design on Montserrat (distance strainmeter to vent >5 km) the possible influence of magma chamber interaction is not reflected in strain data. Thus, simplifying analytical model approaches are valid for strain data inversions.

4. Selected Vulcanian Explosions and Gas Emission Events at Soufrière Hills Volcano Between 2003 and 2012

Volumetric strain changes caused by Vulcanian explosions are often related to pressure variations only in the shallow conduit with decrease in conduit pressure throughout the fragmentation and ejection process (e.g., the 29 July 2008 and the 3 January 2009 explosions reported by *Gottsmann et al*. [2011] and *Chardot et al*. [2010]). This type of event is initiated when gas-rich, crystal-rich magma approaches the surface. As magma ascends and depressurises its viscosity increases due to gas exsolution and microlite crystallization from undercooled melt [*Sparks*, 1997; *Melnik and Sparks*, 1999]. The internal gas pressure within the magma increases and a pressure gradient to the atmosphere is developed. A destabilization of the pressure differential results in a sudden decompression of the magma to atmospheric conditions, initiating a fragmentation wave, which propagates down the conduit causing a Vulcanian explosion [e.g., *Adilbirov and Dingwell*, 1996]. These explosions manifest themselves in the strain data as a sudden deflation (as the explosion empties the upper portion of the conduit), followed by a slower reinflation as the conduit refills with magma ascending from the reservoirs. Cyclic occurrence of this type of Vulcanian explosions as observed at SHV in 1997 (with a series of more than 88 explosions) are attributed to upper conduit processes, such as stick-slip behavior of a stiffend plug that is formed by degassing, melt cooling and crystallization [*Clarke et al*., 2007; *Lensky et al*., 2008], and/or segregation of gas waves in ascending viscous magma due to competition between magma compaction and gas expansion [*Michaut et al*., 2013].

Reassessing strain records from the last decade revealed, however, that a number of Vulcanian explosions and gas emission events at SHV were not associated with changes in just the shallow conduit, but that some events were instead initiated from considerably greater depths and with mechanisms different from those described above. In the following sections, we will present strain data together with corecorded monitoring data from five events that occurred between 2003 and 2012. We will use strain amplitude ratios to infer on the associated pressure evolution within the magmatic system and will discuss the data in regard to the nature of the observed pressure changes.

4.1. Vulcanian Explosions and Gas Emission: 13–16 July 2003

Following a major dome collapse on 12–13 July 2003, a sequence of three Vulcanian explosions occurred between 13 and 15 July 2003. Each explosion created ash columns 11–15 km high [*Herd et al*., 2005] and was followed by 2–4 h of ash venting and low-amplitude seismic tremor. *Herd et al*. [2005] inferred a volume of 10^6 m^3 of erupted DRE (Dense Rock Equivalent) for the final explosion on 15 July. The strain data recorded throughout the first two events indicate pressure changes in the shallow conduit only, however, strain data from the final Vulcanian explosion that took place on 15 July 2003 at 5:29 (all times are given in UTC) showed that dynamics in the active plumbing system of SHV had changed fundamentally. All three explosions show similar signals for the first ~100 s with maximum negative strain amplitudes of 25 nS at AIRS and a ratio of strains for AIRS/TRNT = 2, which is best modeled by a sudden pressure reduction in a 1.5 km deep cylindrical conduit. This is consistent with an erupted volume of 10^6 km^3 estimated by *Herd et al*. [2005], equivalent to emptying a 15 m radius conduit to a depth of about 1.4 km. While the explosions on the 13 and 14 July show a strain recovery of about 50% that reflects the refill of the conduit over a period of approximately 20 min, the eruption on the 15 July was followed by a large overrecovery (200%) over a period of 90 min with negative strain changes (i.e., contraction) of 58 nS at AIRS and 81 nS at TRNT (Figure 4a). The amplitude ratios of AIRS/TRNT = 0.7 during recovery suggests an additional involvement of the deeper magmatic system, in particular, a simultaneous decompression of the LMC + UMC together with a pressurization of the shallow dyke. In order to infer absolute pressure changes from strain amplitudes we use seismic *P*-wave velocities to constrain the properties of the upper crust [*Paulatto et al*., 2010]. We apply the function of *Brocher* [2005] to infer seismic *S*-wave velocities and densities and a standard relationship [*Wang*, 2000] to convert dynamic into static values of the Young's Modulus *E* (see *Hautmann et al*. [2013] for details). Resulting values for E_S are increasing linearly with depth from 6 GPa (at the surface) to 25 GPa (≥6 km depth). The Poisson's ratio is $\nu = 0.25$. Based on these crustal properties, we infer that the pressure

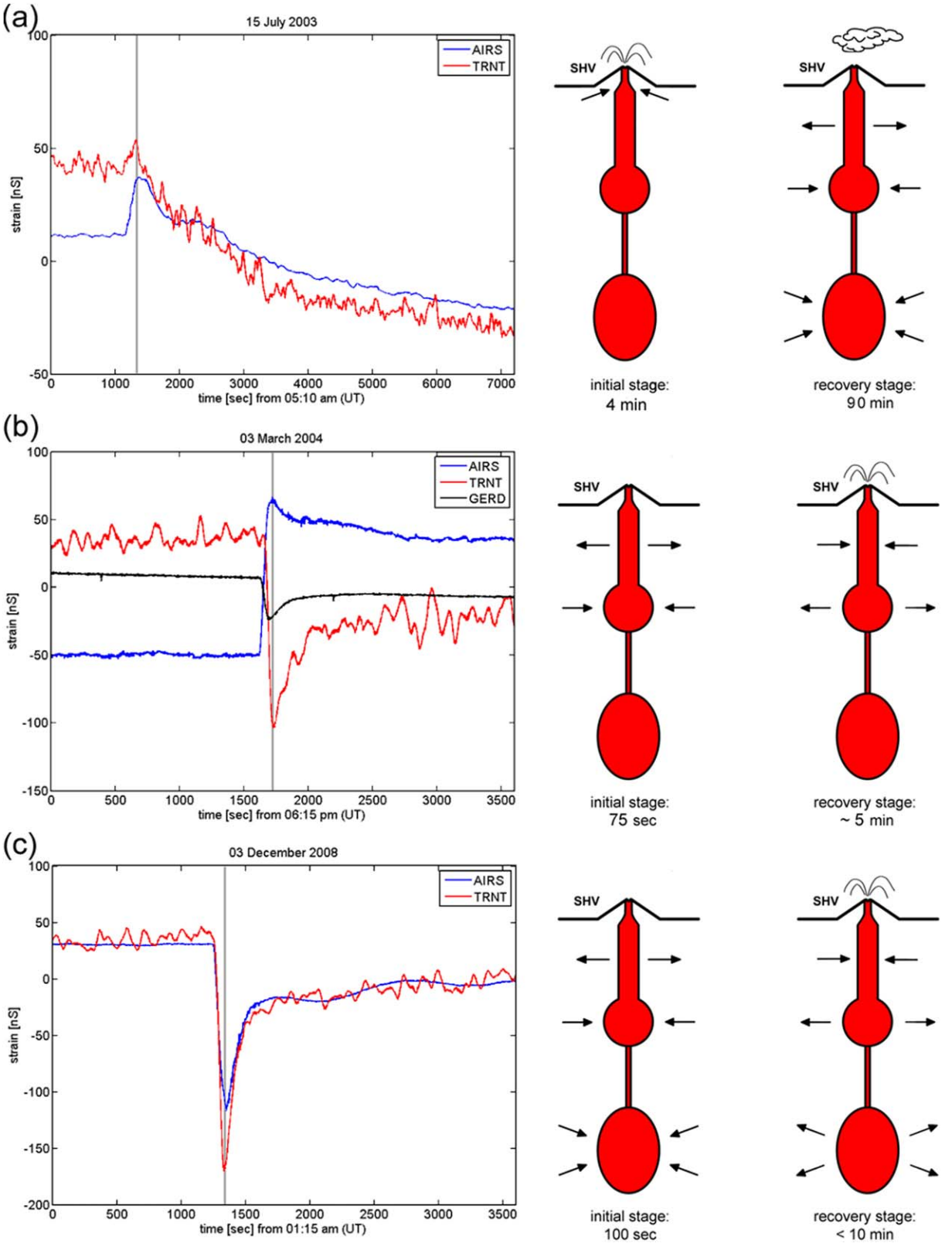

Figure 4. Strain data recorded during Vulcanian explosions at Soufrière Hills Volcano on (a) 15 July 2003, (b) 3 March 2004, and (c) 3 December 2008. All events were preceded by an initial stage that lasted between 1 and 4 min. Strain signals peaked with the onset of the explosion (indicated by gray bar) and the system subsequently recovered for up to 90 min. We used strain ratios to infer-related pressure changes in the magmatic system (shown in the sketches on the right). The short time scales for the pressure changes hint toward rapid ascent of gas rather than magma as source of pressure changes.

changes associated with the strain signals from 15 July 2003 were approximately −0.3 MPa within LMC + UMC and +0.3 MPa within the shallow dyke. The gas emission that was associated with the Vulcanian eruptions could not be measured because the eruption of volcanic ash scattered the ultra-violet light that is used to detect SO_2 [*Edmonds and Herd*, 2007]. However, on the 16 July 2003 increased gas emission was observed at SHV. The absence of ash during this event allowed accurate measurement of the SO_2 released by DOAS and this comprised a release of 1×10^5 kg SO_2 over approximately 1 h, at a mean rate of 28 kg/s [*Edmonds and Herd*, 2007]. For comparison, the mean background degassing rate for SO_2 for that day was 3.2 kg/s.

We can summarize that the dome collapse on 12 July 2003 depressurized the shallow plumbing system within SHV, leading to a flow of magma from depth toward the surface. The Vulcanian explosions of the 13, 14, and 15 July resulted from a sudden decompression of the high pressure, vesiculated magma that led to a fragmentation of magma in the shallow conduit [*Voight et al*., 2010]. The explosions on 13 and 14 July were followed by a refill of the shallow conduit probably as a consequence of vesiculation of the magma in the chamber with the pressure remaining constant in the UMC. The final explosion on 15 July marked the onset of pressure changes deeper within the magmatic system. The strain data indicate a contraction of both magma chambers (LMC + UMC) together with a filling of the upper dyke-conduit. The signal can be linked to the ascent of either magma or magmatic fluids from the storage centres into the shallow plumbing system. However, the short timescale of the response (approx. 90 min) of the LMC + UMC are more easily explained by magmatic fluids than by high viscosity magma. Accumulated gases in the shallow plumbing system were then released to the surface in a slow, prolonged degassing event. The gas emission detected on the 16 July was possibly part of the latter stage of this degassing.

4.2. Vulcanian Explosion: 3 March 2004

The explosion on 3 March 2004 at 18:45 followed a long-period seismic swarm and tremor during an episode of relative volcanic quiescence and dome growth cessation that began after the major dome collapse in July 2003. The explosion removed a small dome and generated an ash plume about 7 km high. The volume of erupted DRE was inferred from the plume height and estimated as 5.1×10^4 m^3 [*Linde et al*., 2010]. The DOAS network recorded SO_2 emission on 3 and 5 March 2004 at a level that was moderately above-average with approximately 825 t/d (9.5 kg/s). Corecorded strain data show a rapid initial phase during which AIRS experienced expansion of 115 nS, while TRNT and GERD underwent 140 and 30 nS contraction, respectively (Figure 4b). The observations and inferred strain ratios were interpreted by *Linde et al*. [2010] as a simultaneous contraction of the UMC and expansion of the dyke-conduit. The amplitudes of the strain signals correspond to pressure changes of about 2.5 MPa (i.e., 2.5 MPa pressure decrease in the magma chamber and 2.5 MPa pressure increase in the shallow dyke). The initial stage before the explosion lasted about 75 s and was followed by a phase of pressure recovery of the system by 50% (partial dyke closure and partial reinflation of the UMC) that lasted another ∼300 s and was accompanied by pyroclast ejection and plume formation.

The Vulcanian explosion on 3 March 2004 was preceded over a 75 s period by a deflation of the UMC with a simultaneous opening of the shallow dyke. It is, therefore, the first documented event that is characterized by the involvement of the magmatic storage region and the shallow plumbing system in both the initial and the recovery phase (Figure 4b). Because the pressure changes occur over periods of a few minutes, we infer that inviscid gas rather than high viscosity magma transfer from the deeper storage centre into the dyke drives the observed pressure changes. We thus propose that magmatic fluids (gas at shallow levels) ascended from the UMC and accumulated in the shallow dyke-conduit system leading to an overpressure buildup that is released with the beginning of the eruption. This hypothesis is in agreement with seismic data interpretation from *Green and Neuberg* [2005], who inferred that the shallow magmatic system was pressurized by a trapped gas phase before the start of the 3 March 2004 eruption.

4.3. Vulcanian Explosion: 3 December 2008

The explosion on 3 December 2008 at 1:37 was the first and largest event in a series of explosive eruptions that took place between 3 and 5 December. The explosions marked the end of an episode of relative volcanic quiescence and dome growth stagnation and preceded a 1 month long lava extrusion event. Activity onset on 3 December was marked by a small dome collapse, which was followed by a pyroclastic flow. Within 90 s there was one, possibly two explosions with ballistic ejections of mainly dome-rock lithics

involving at a total volume of $\sim 1.2 \times 10^6$ m^3 DRE [*Komorowski et al*., 2010]. The explosion and associated pyroclastic flows generated ash columns up to a height of 12 km. Unfortunately, the strainmeter at GERD was not operating during the Vulcanian explosion. However, the records from the remaining sites AIRS and TRNT show contractions of 146 and 210 ns, respectively (i.e., AIRS/TRNT ratio 0.7; Figure 4c), which equals the ratio that was identified for coupled dynamics in the entire magmatic system with a deflation of the two magma chambers (LMC + UMC) and a dilation of the shallow dyke-conduit. The initial contraction phase lasted about 100 s and was followed by a 70% recovery of the system that lasted less than 10 min. Associated pressure changes are calculated at ~1 MPa. The following three explosive events were markedly smaller than the first. Corecorded strain data showed deflation at AIRS and TRNT between 4 and 6 ns, which typically relate to conduit only fragmentation events. Due to equipment malfunction, the SO_2 flux could only be measured between 9 and 12 December, where an average flux of 402 t/d (equals 4.6 kg/s) was recorded, which reflects typical background activity at the volcano.

Based on recorded strain amplitude ratios we infer that the entire magmatic system, including the LMC, was affected by the pressure changes before/after the 3 December 2008. The explosion was preceded by a short (100 s lasting) initial phase of LMC + UMC depressurization and simultaneous dyke opening. Given the short duration of the initial stage, the pressure changes are inferred to be caused by the ascent of magmatic fluids from the magma chambers into the dyke. In contrast, strain data from the subsequent explosions between 3 and 5 December 2008 indicate that pressure changes occurred only in the upper conduit, which supports the assumption that these events were triggered when the preceding minor dome collapse exposed regions of hot, gas-pressurized lava [*MVO*, 2008].

On 8 December 2008, a 1 month lasting period of very fast extrusion of andesite resumed at SHV [*Komorowski et al*., 2010]. Corecorded strain data from this period document that this event was associated with a similar pressure evolution in the magmatic system than the 3 December 2008 Vulcanian explosion (LMC + UMC decompression, dyke compression). The pressure changes in the magmatic system were interpreted with a rapid ascent of deeper-seated magma into the shallow plumbing centre and partly further up to the surface [*Hautmann et al*., 2013].

4.4. Pressure Changes: 19 August 2010

On 19 August 2010 strain dilatometers documented a small cluster of pressure changes in the magmatic system, between 14:00 and 16:00, which, however, were not associated with volcanic surface activity or changes in seismicity or gas emission. The strain event took place in a time of volcanic quiescence after a major dome collapse in February 2010. The initial signal reflects an overall system contraction at small magnitude only with 40 nS recorded at AIRS, 45 nS at TRNT, and 9 nS at GERD (Figure 5a). The AIRS/TRNT ratio of 0.9 indicates once more the decompression of the two magma chambers by <0.5 MPa and the simultaneous dilation of the shallow dyke. The initial stage and the recovery phase of the event both lasted about 25 min. During the recovery phase all sites showed expansion at a maximum of 24 nS at AIRS, however, the observed strain ratios AIRS/TRNT = 1.1 and AIRS/GERD = 2 indicate inflation of the LMC only.

The August 2010 event is particularly interesting, as the strain dilatometers were the only instruments to detect dynamics in the magmatic system of SHV during a time of apparent volcanic quiescence. The recorded signals most likely result from ascent of magmatic fluids from the two magma chambers (LMC + UMC) into the upper dyke. In contrast to earlier events, strain data from the recovery phase indicate reinflation of only the LMC. As the pressure changes were lacking associated vent activity including above-average gas emission, we assume that the gas, which ascended into the shallow plumbing system, was not able to escape at the surface as the pressure buildup was not sufficient to break the conduit plug. The low amplitude of the pressure changes (45 nS at maximum, compared to 150–320 nS during other events) supports this hypothesis. It seems, therefore, likely that the ascending magmatic fluids were stored in the shallow dyke (Figure 5a), explaining (i) the absence of increased gas emission after the strain event and (ii) missing dyke deflation in the recovery phase.

4.5. Gas Emission: 22–23 March 2012

The most recent short-term volcanic activity associated with pressure changes in the deeper magmatic system was an ash venting/gas emission event that occurred on 22–23 March 2012. At this time SHV had been quiescent for almost 2 years with no lava dome extrusion and only low seismic activity and small deformational changes indicating a slow refilling of the reservoirs [*MVO report to the SAC 17*, 2012]. The event was induced by

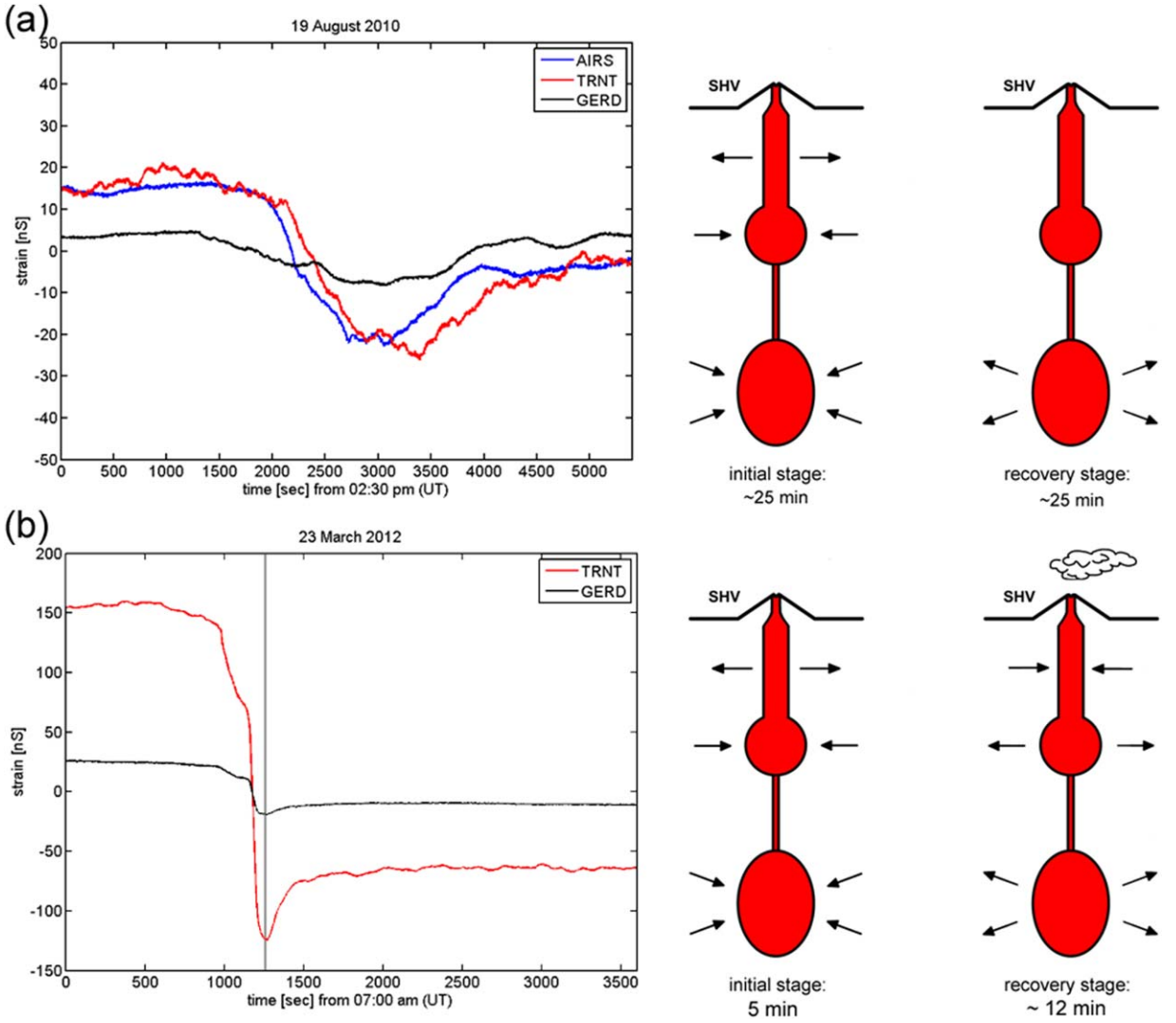

Figure 5. Strain changes at Soufrière Hills Volcano recorded on (a) 19 August 2010 and (b) 23 March 2012. While the first event (a) was expressed in strain data but not accompanied by surface activity, the second event (b) was accompanied by gas emission and ash venting (its onset is indicated by the gray bar). Strain ratios were used to infer on related source activity in the magmatic system. The time scales for pressure changes before/after each event (25 min at maximum for initial stage and recovery stage) suggest gas rise rather than magma movement to initiate the pressure changes in the magmatic system.

two intense strings of VT earthquakes that peaked in a M_L 3.9 VT and three large hybrid events terminating the swarm on 23 March 2012 at 7:20. Strain data document that pressure rise was initiated from the magmatic system about 300 s before the M_L 3.9 event and continued for another 60 s afterward. The maximum amplitude of strain was 280 nS at TRNT and 45 nS at GERD (AIRS was not operating at that time; Figure 5b). The strain data (TRNT/GERD 6.4) indicate a joint LMC + UMC inflation and dyke deflation with pressure changes of 1.3 MPa. The entire system recovers (LMC + UMC deflation, dyke inflation) by 23% during the following 10 min. Within 2 h of the termination of the seismic swarms volcanic surface activity in form of ash venting and steam degassing began. Between 23 and 27 March 2012 increased rate of SO_2 degassing was measured by the OMI satellite with a peak of over 5200 t/d (60 kg/s) on 24 March [*MVO report to the SAC 17*, 2012]. Elevated gas emission was also confirmed by the DOAS network on 24 and 26 March (peaking on the 26 March at 4600 t/d (53 kg/s), which is the third highest level measured by DOAS since 2002 [*MVO report to the SAC 17*, 2012]).

The 23 March 2012 gas emission and ash venting event was initiated by a deflation of the two magma chambers together with a dilation of the shallow dyke, followed by reverse dynamics in the recovery phase (Figure 5b). Given the short time scales of a few minutes for pressurization/depressurization of the magmatic system, we again consider magmatic fluid ascent from the deeper magmatic system into the shallow

dyke to play a major role in the initiation of this event. Once the overpressures in the shallow dyke exceeded a critical threshold, gas leak at the surface started and continued for another 3–4 days as documented in the gas emission records. The pressure evolution within the magmatic system (initial stage and recovery phase) was similar to the pressure changes identified for the 3 December 2008 explosion (see section 4.3). Also the magnitude of pressure changes and the duration of initial/recovery phases were similar for both events.

5. Interpretation and Implications

The new data document for the first time the ascent of magmatic fluids from deep within a major magmatic system that can, in some cases, be unrelated to magma ascent. Recorded strain changes indicate a decompression of either the UMC or both magma chambers (LMC + UMC) together with a simultaneous dilation of the plumbing dyke prior to the analyzed eruptive events. The timescales involved (typically minutes) are far too short to be associated with magma transport over depths of several kilometers. Therefore, we infer that magmatic fluid is being released and rises from pockets in the deeper storage system. We interpret the observations as transport of volatiles from the magma chambers into the shallow dyke, leading to an overpressure buildup that—when overcoming the gravitational load and structural resistance of the conduit plug—results in a Vulcanian eruption or a discrete gas emission event. The subsequent recovery phase in the strain data corresponds to the release of gas from the shallow dyke to the surface, while the partial reinflation in the storage system might correlate to an expansion of compressed gases due to released pressure.

We consider two scenarios that can initiate a deflation of the two vertically stacked magma chambers: (i) The LMC and UMC are a fully connected system and gas release from only the UMC results in pressure changes in both magma chambers. (ii) A new pathway for dynamic gas ascent is created from the LMC to the UMC each time the UMC connects to the surface. Based on the available data, we cannot prefer one model over the other. However, the first scenario seems more likely as it does not require an interconnected chain of magma embedded fluid pockets and gas is only released from the UMC. Fluids from deep within the magmatic system are carbon dioxide and sulphur rich, but water and chlorine poor, while due to solubility relationships shallow magmatic fluids are richer in water and chlorine [*Edmonds et al*., 2014]. It is known that the SO_2/HCl ratio changes significantly during dome growth [*Edmonds et al*., 2002] when magma ascends from the UMC and highly soluble water and chlorine degas during magma rise within the dyke-conduit. Although a similar effect can be expected for gas release from deeper within the magmatic system (with the LMC releasing gas richer in S and CO_2 than the UMC), assessing LMC versus UMC contribution during Vulcanian eruptions remains difficult.

The rise of fluids within tens to hundreds of seconds in a magmatic system that extends toward midcrustal depths requires fast fluid pathways. Many of the well-established processes of gas transport, for example bubble rise and shear fracturing, seem hard to reconcile with the time scales and depths of the observed pressure changes. Melt compositions in the SHV andesite are rhyolitic and, assuming water-saturation, viscosities are of the order 10^5-10^6 Pa s at 850°C [*Hess and Dingwell*, 1996; *Sparks et al*., 2000]. If the typical bubble diameters were 1 mm then Stokes rise velocities are of order 10^{-8} to 10^{-9} m/s, which is 9–10 orders of magnitude greater than the velocities implied by the data. As such bubble rise cannot account for the ascent of volatiles causing the observed pressurization of the dyke. Permeable flow of gas through interconnected networks of either bubbles [*Okumura et al*., 2008] or fractures formed from shear forces [*Caricchi et al*., 2011; *Cordonnier et al*., 2012] is also considered as effective mechanisms for network formation that facilitates effective degassing [e.g., *Gonnermann and Manga*, 2003; *Caricchi et al*., 2011]. Critical conditions for magma to rupture are, however, only reached at relatively shallow depths (about 1500 m), where the magma viscosity increases due to melt dehydration [*Sparks*, 1997; *Neuberg et al*., 2006]. Shear fracturing and faulting of magma seems, therefore, not viable for the formation of fluid pathways deep within the magmatic system. Although movement through a permeable network of interconnected bubbles is a possible transport mechanism also at larger depths [*Okumura et al*., 2009], the permeabilities needed to transport gas at several m/s are not plausible. For system permeabilities between 10^{-10} and 10^{-15} m^2, which is similar to the permeabilities inferred for the SHV upper magmatic system [*Edmonds et al*., 2003], *Okumura et al*. [2009] experimentally obtain gas velocities in the range $10^{-5}-10^{-3}$ m/s.

One viable mechanism of rapid fluid transport, that is well known from studies of ore deposits [*Sillitoe*, 2010] and kimberlites [*Sparks et al*., 2006], is the formation of networks of tensile hydraulic fractures that are

large enough to transport low viscosity (inviscid) fluids at the required speeds. Applying the theory developed by *Lister and Kerr* [1991], *Sparks et al.* [2006] estimated typical speeds of fluid-filled propagating fractures to be in the range 5 to 20 m/s in the inviscid (high Reynolds number regime). Although this application was for kimberlite magmas they apply equally well to magmatic fluids since the only relevant properties are buoyancy and very low viscosity.

Earthquakes are not recorded in association with the events except in the shallow crust, so a significant part of the fluid transport process is either aseismic or that the seismicity is undetectable. Hydraulic fractures in cold brittle rock would be expected to induce seismicity. However, the pathways in the SHV magma system are formed in hot ductile rock, which may contain partial melt. If small earthquakes were formed then the energy may be unable to escape through a crystalline melt-mush system.

The sudden onset of the fluid ascent events, together with the fast ascent speeds imply that large pockets of already segregated fluid existed in the magmatic system and were released by rapid destabilization. How could such pockets arise? Recent research on deep fluids and melts has highlighted the role of compaction in segregating both fluids and melts from crystalline materials into lenses [*Solano et al.*, 2012; *Connolly and Podladchikov*, 2013]. The physics of the segregation process of magmatic fluids likely involves exsolution from volatile-saturated melts, bubble rise and coalescence into pockets of fluid. The formation of melt and fluid lenses is a very slow process as it is governed by the very high viscosity of the crystalline matrix, but the length scales of melt or fluid lenses and timescales are also governed by melt or fluid viscosity and buoyancy relative to the matrix. Given that melts and fluids have very different viscosities and densities it is expected that, once exsolved, fluids and melts can become decoupled and segregate. Thus, the concept of large pockets of magmatic fluid that can then become unstable to form fast pathway fractures may help explain the observations. The gas segregation by compaction will produce horizontal layers, which, however, not hamper fluid transport in vertical direction. The horizontal layers are intrinsically unstable and theoretical studies indicate that in porous media these can transform into vertically oriented fingers or channels as well as destabilizing to form fast-transfer fluid-filled cracks [*Connolly and Podladchikov*, 2013].

After the expulsion of the gas phase the fracture system subsequently relaxed and healed due to (i) cohesion between surfaces of adjacent particles and (ii) viscous deformation that fills pore spaces between imperfectly packed particles [*Sparks et al.*, 1999; *Tuffen et al.*, 2003]. The annealing time of the fractures after the removal of gas can be calculated using the Maxwell relationship, i.e., the fractures will heal over a duration equal to the relaxation time of the melt-crystal system:

$$t_{relax} = \eta / G_{\infty} \quad (1)$$

where η is the Newtonian viscosity of the magma and G_{∞} is the shear modulus at infinite frequency (10^{10} Pa). Considering rather high magma viscosities of 10^{9} Pa s, as was inferred for degassed melts in the shallow plumbing system [*Melnik and Sparks*, 2002], we deduce an immediate relaxation of the system that implies a rapid healing of fractures. Although the time that cracks remain open is additionally controlled by the amount of gas that escapes the system [*Cordonnier et al.*, 2012], we infer that an interconnected fracture system is only short-lived and not preserved for the time period between individual explosion events at SHV, but that a new path is formed prior to each event.

6. Conclusions

Interrogation of strain data from three Sacks-Evertson borehole strainmeters located on the flanks of Soufrière Hills Volcano (Montserrat, W.I.) allows us to quantify pressure changes in the active magmatic system during discrete and short-lived volcanic eruption events. We presented a literature review that summarizes strain observations and modeling results published since the installation of strainmeters on Montserrat about 10 years ago. We show that pressure changes in each of the segments of the SHV active magmatic system generate a characteristic pattern in the strain field with a unique amplitude ratio of strains between the sampling sites. The results enabled us to infer a simple scheme that offers an immediate approach to correlate strain records with the operating sources in the subsurface.

Our findings enabled us to identify a number of Vulcanian explosions and gas emission events at SHV that were clearly not driven by conduit dynamics in just the shallow edifice but by pressure release deep within

the magmatic system. As such, our study provides the rare opportunity to apply geodetic observables for assessing magma chamber dynamics that are commonly approached by petrologic observations and theoretical models. The strain data indicate that these events relate to a rapid contraction— in tens to hundreds of seconds—of either one or two magma chambers along with an inflation of the shallow dyke-conduit system. We interpret this observation as due to the rise of magmatic fluids from pockets in the magma chambers into the plumbing system. Such rapid ascent of magmatic fluids is incompatible with bubble rise, bubble coalescence, and shear fracturing and we ascribe permeable flow through networks of tensile hydraulic fractures as the only viable transport mechanism. Formation of fluid supplied vein networks in high grade metamorphic and igneous systems also require segregation of large amounts of fluid that are then released suddenly to form veins [*Connolly and Podladchikov*, 2013]. It is possible that such events expected from geological evidence and predicted from theory are being witnessed at SHV.

Acknowledgments

SH acknowledges support from the German National Academy of Sciences Leopoldina (LPDS 2009-47), RSJS thanks a European Research Council grant (VOLDIES project; grant agreement n° 228064) and FW acknowledges support by a NERC grant (NE/F004222/1). We wish to thank the staff of the Montserrat Volcano Observatory and the CALIPSO project, in particular B. Voight and G.S. Mattioli, for deploying and maintaining the network of strainmeters across Montserrat. G. Wadge is thanked for his careful review that improved the manuscript.

References

Adilbirov, M. A. and D.B. Dingwell (1996), Magma fragmentation by rapid decompression, *Nature*, *380*, 146–148.

Annen, C., J. D. Blundy, and R. S. J. Sparks (2006), The genesis of intermediate and silicic magmas in deep crustal hot zones, *J. Petrol.*, *47*(3), 505–539, doi:10.1093/petrology/egi084.

Annen, C., M. Paulatto, R. S. J. Sparks, T. A. Minshull, and E. J. Kiddle (2014), Quantification of the intrusive Magma fluxes during magma chamber growth at Soufrière Hills Volcano (Montserrat, Lesser Antilles), *J. Petrol.*, *55*(3), 529–548, doi:10.1093/petrology/egt075.

Aspinall, W. P., A. D. Miller, L. L. Lynch, J. L. Latchman, R. C. Stewart, R. A. White, and J. A. Power (1998), Soufriére Hills eruption, Montserrat, 1995–1997: Volcanic earthquake locations and fault plane solutions, *Geophys. Res. Lett.*, *25*, 3397–3400.

Barclay, J., M. J. Rutherford, M. R. Carroll, M. D. Murphy, J. D., Devine, J. Gardner, and R. S. J. Sparks (1998), Experimental phase equilibria constraints on pre-eruptive storage conditions of the Soufrière Hills magma, *Geophys. Res. Lett.*, *25*, 3437–3440.

Brocher, T. M. (2005), Empirical relations between elastic wavespeeds and density in the earth's crust, *Bull. Seismol. Soc. Am.*, *95*, 2081–2092, doi:10.1785/0120050077.

Caricchi, L., A. Pommier, M. Pistone, J. Castro, A. Burgisser, and D. Perugini (2011), Strain induced magma degassing: Insights from simple-shear experiments on bubble bearing melts, *Bull. Volcanol.*, *73*(9), 1245–1257.

Chardot, L., et al. (2010), Explosion dynamics from strainmeter observations, Soufrière Hills Volcano, Montserrat, W.I.: 2008–2009, *Geophys. Res. Lett.*, *37*, L00E24, doi:10.1029/2010GL044661.

Clarke, A. B., S. Stephens, R. Teasdale, R. S. J. Sparks, and K. Diller (2007), Petrological constraints on the decompression history of magma prior to Vulcanian explosions at the Soufrière Hills volcano, Montserrat, *J. Volcanol. Geotherm. Res.*, *161*, 261–274.

Connolly, J. A. D., and Y. Y. Podladchikov (2013), A hydromechanical model of lower crustal fluid flow, in *Metasomatism and the Chemical Transformation of Rock, Lect. Notes Earth Syst. Sci.*, edited by D. E. Harlov and H. Austrheim, pp. 599–658, Springer-Verlag, Heidelberg, doi:10.1007/978-3-642-28394-9_14.

Cordonnier, B., L. Caricchi, M. Pistone, J. Castro, K.-U. Hess, S. Gottschaller, M. Manga, D. B. Dingwell, and L. Burlini (2012), The viscous-brittle transition of crystal-bearing silicic melt: Direct observation of magma rupture and healing, *Geology*, *40*, 611–614, doi:10.1130/G3914.1.

Costa, A., O. Melnik, R. S. J. Sparks, and B. Voight (2007), Control of magma flow in dykes on cyclic lava dome extrusion, *Geophys. Res. Lett.*, *34*, L02303, doi:10.1029/2006GL027466.

Devine, J. D., M. D. Murphy, M. J. Rutherford, J. Barclay, R. S. J. Sparks, M. R. Carroll, S. R. Young, and J. E. Gardner (1998), Petrologic evidence for pre-eruptive pressure-temperature conditions, and recent reheating of andesitic magma erupting at the Soufrière Hills Volcano, Montserrat, W.I, *Geophys. Res. Lett.*, *25*, 3669–3672, doi:10.1029/98GL01330.

Edmonds, M., and R. A. Herd (2007), A volcanic degassing event at the explosive-effusive transition, *Geophys. Res. Lett.*, *34*, L21310, doi:10.1029/2007GL031379.

Edmonds, M., D. M. Pyle, and C. Oppenheimer (2001), A model for degassing at the Soufrière Hills Volcano, Montserrat, West Indies, based on geochemical data, Earth Planet. *Sci. Lett.*, *186*, 159–173.

Edmonds, M., D. M. Pyle, and C. Oppenheimer (2002), HCl emissions at Soufrière Hills Volcano, Montserrat, West Indies, during a second phase of dome building: November 1999 to October 2000, *Bull. Volcanol.*, *64*, 21–30, doi:10.1007/s00445-001-0175-0.

Edmonds, M., C. Oppenheimer, D. M. Pyle, R. A. Herd, and G. Thompson (2003), SO2 emissions from Soufrière Hills Volcano and their relationship to conduit permeability, hydrothermal interaction and degassing regime, *J. Volcanol. Geotherm. Res.*, *124*(1–2), 23–43, doi:10.1016/S0377-0273(03)00041-6.

Edmonds, M., et al. (2014), Pre-eruptive vapor and its role in controlling eruption style and longevity at Soufrière Hills Volcano, in *The Eruption of Soufrière Hills Volcano, Montserrat, From 2000 to 2010, Geol. Soc. Mem.*, vol. *39*, edited by G. Wadge, R., Robertson, and B. Voight, 289–313, doi:10.1144/M39.16, Geol. Soc., London.

Elsworth, D., G. Mattioli, J. Taron, B. Voight, and R. Herd (2008), Implications of magma transfer between multiple reservoirs on eruption cycling, *Science*, *322*, 246–248, doi:10.1126/science.1161297.

Formenti, Y., T. H., Druit, and K. Kelfoun (2003), Characterisation of the 1997 Vulcanian explosions of Soufrière Hills Volcano, Montserrat, by video analysis, *Bull. Volcanol.*, *65*, 587–605, doi:10.1007/s00445-003-0288-8.

Gonnermann, H. M., and M. Manga (2003), Explosive volcanism may not be an inevitable consequence of magma fragmentation, *Nature*, *426*, 432–435, doi:10.1038/nature02138.

Gottsmann, J., S. De Angelis, N. Fournier, M. Van Camp, S. Sacks, A. Linde, and M. Ripepe (2011), On the geophysical fingerprint of Vulcanian explosions, *Earth Planet. Sci. Lett.*, *306*, 89–104, doi:10.1016/j.epsl.2011.03.035.

Green, D. N., and J. Neuberg (2005), Seismic and infrasonic signals associated with an unusual collapse event at the Soufrière Hills Volcano, Montserrat, *Geophys. Res. Lett.*, *32*, L07308, doi:10.1029/2004GL022265.

Hautmann, S., J. Gottsmann, R. S. J. Sparks, A. Costa, O. Melnik, and B. Voight (2009), Modelling ground deformation caused by oscillating overpressure in a dyke conduit at Soufrière Hills Volcano, Montserrat, *Tectonophysics*, *471*, 87–95, doi:10.1016/j.tecto.2008.10.021.

Hautmann, S., J. Gottsmann, R. S. J. Sparks, G. S. Mattioli, I. S. Sacks, and M. H. Strutt (2010), Effect of mechanical heterogeneity in arc crust on volcano deformation with application to Soufrière Hills Volcano, Montserrat, West Indies, *J. Geophys. Res.*, *115*, B09203, doi:10.1029/2009JB006909.

Hautmann, S., D. Hidayat, N. Fournier, A. T. Linde, I. S. Sacks, and C. P. Williams (2013), Pressure changes in the magmatic system during the December 2008/January 2009 extrusion event at Soufrière Hills Volcano, Montserrat (W.I.), derived from strain data analysis, *J. Volcanol. Geotherm. Res.*, *250*, 34–41, doi:10.1016/j.jvolgeores.2012.10.006.

Herd, R. A., M. Edmonds, and V. A. Bass (2005), Catastrophic lava dome failure at Soufriere Hills Volcano, Montserrat, 12–13 July 2003, *J. Volcanol. Geotherm. Res.*, *148*, 234–252, doi:10.1016/j.jvolgeores.2005.05.003.

Hess, K.-U., and D. B. Dingwell (1996), Viscosities of hydrous leucogranitic melts: A non-Arrhenian model, *Am. Mineral.*, *81*, 1297–1300.

Komorowski, et al. (2010), Insights into processes and deposits of hazardous vulcanian explosions at Soufrière Hills Volcano during 2008 and 2009 (Montserrat, West Indies), *Geophys. Res. Lett.*, *37*, L00E19, doi:10.1029/2010GL042558.

Lensky, N. G., R. S. J. Sparks, O. Navon, and V. Lyakhovsky (2008), Cyclic activity at Soufrière Hills volcano, Montserrat, in *Fluid Motions in Volcanic Conduits: A Source of Seismic and Acoustic Signals*, vol. *307*, edited by S. J. Lane and J. S. Gilbert, pp. 169–188, Geol. Soc., Spec. Publ., London.

Linde, A. T., et al. (2010), Vulcanian explosion at Soufrière Hills Volcano, Montserrat on March 2004 as revealed by strain data, *Geophys. Res. Lett.*, *37*, L00E07, doi:10.1029/2009GL041988.

Lister, J. R., and K. C. Kerr (1991), Fluid-mechanical models of crack propagation and their application to magma transport in dykes, *J. Geophys. Res.*, *96*, 10,049–10,077.

Mattioli, G., T. H. Dixon, F. F. Farina, E. S. Howell, P. E. Jansma, and A. L. Smith (1998), GPS measurement of surface deformation around Soufrière Hills Volcano, Montserrat, from October 1995 to July 1996, *Geophys. Res. Lett.*, *25*, 3417–3420, doi:10.1029/98GL00931.

Melnik, O., and A. Costa (2014), Dual chamber-conduit models of non-linear dynamics behaviour at Soufrière Hills Volcano, Montserrat, in *The Eruption of Soufrière Hills Volcano, Montserrat, From 2000 to 2010, Geol. Soc. Mem.*, vol. *39*, edited by G. Wadge, R., Robertson, and B. Voight, 61–69, doi:10.1144/M39.3, Geol. Soc., London.

Melnik, O., and R. S. J. Sparks (1999), Nonlinear dynamics of lava dome extrusion, *Nature*, *402*, 37–41.

Melnik, O., and R. S. J. Sparks (2002), Dynamics of magma ascent and lava extrusion at Soufrière Hills Volcano, Montserrat, in *The Eruption of Soufrière Hills Volcano, Montserrat, From 1995 to 1999, Geol. Soc. Mem.*, vol. *21*, edited by T. H. Druitt and B. P. Kokelaar, pp. 153–172, Geol. Soc., London.

Michaut, C., Y. Ricard, D. Bercovici, and R. S. J. Sparks (2013), Eruption cyclicity at silicic volcanoes potentially caused by magmatic gas waves, *Nat. Geosci.*, *6*, 856–860, doi:10.1038/NGEO1928.

Murphy, M. D., R. S. J. Sparks, J. Barclay, M. R. Carroll, and T. S. Brewer (2000), Remobilization of andesite magma by intrusion of mafic magma at the Soufrière Hills Volcano, Montserrat, West Indies, *J. Petrol.*, *41*(1), 21–42, doi:10.1093/petrology/41.1.21.

MVO (2008), Montserrat Volcano Observatory, Weekly activity reports, open file reports. [Available at: http://www.mvo.ms.].

MVO report to the SAC 17 (2012), Open file report. [Available at: http://www.mvo.ms.].

Neuberg, J. W., H. Tuffen, L. Collier, D. Green, T. Powell, and D. Dingwell (2006), The trigger mechanism of low-frequency earthquakes on Montserrat, *J. Volcanol. Geotherm. Res.*, *153*, 37–50.

Okumura, S., M. Nakamura, A. Tsuchiyama, T. Nakano, and K. Uesugi (2008), Evolution of bubble microstructure in sheared rhyolite: Formation of a channel-like bubble network, *J. Geophys. Res.*, *113*, B07208, doi:10.1029/2007JB005362.

Okumura, S., M. Nakamura, S. Takeuchi, A. Tsuchiyama, T. Nakano, and K. Uesugi (2009), Magma deformation may induce non-explosive volcanism via degassing through bubble networks, *Earth Planet. Sci. Lett.*, *281*, 267–274, doi:10.1016/j.epsl.2009.02.036.

Pascal, K., J. Neuberg, and E. Rivalta (2012), On precisely modelling surface deformation due to interacting magma chambers and dykes, *Geophys. J. Int.*, *196*, 253–278, doi:10.1093/gji/ggt343.

Paulatto, M., et al. (2010), Upper crustal structure of an active volcano from refraction/reflection tomography, Montserrat, Lesser Antilles, *Geophys. J. Int.*, *180*, 685–696, doi:10.1111/j.1365-246X.2009.04445.x.

Paulatto, M., C. Annen, T. J. Henstock, E. Kiddle, T. A. Minshull, R. S. J. Sparks, and B. Voight (2012), Magma chamber properties from integrated seismic tomography and thermal modeling at Montserrat, *Geochem. Geophys. Geosyst.*, *13*, Q01014, doi:10.1029/2011GC003892t.

Sillitoe, R. (2010), Porphyry copper deposits, *Econ. Geol.*, *105*, 3–41, doi:10.2113/gsecongeo.105.1.3.

Solano, J. M. S., M. D. Jackson, R. S. J. Sparks, J. D. Blundy, and C. Annen (2012), Impact of melt segregation on the genesis of intermediate and silicic magmas in deep crustal hot zones, *J. Petrol.*, *53*, 1999–2026, doi:10.1093/petrology/egs041.

Sparks, R. S. J. (1997), Causes and consequences of pressurisation in lava dome eruptions, *Earth Planet. Sci. Lett.*, *150*, 177–189.

Sparks, R. S. J., S. R. Tait, and Y. Yanev (1999), Dense welding caused by volatile resorption, *Geol. Soc. J.*, *156*, 217–225.

Sparks, R. S. J., M. D. Murphy, A. M. Lejeune, R. B. Watts, J. Barclay, and S. R. Young (2000), Control on the emplacement of the andesite lava dome of the Soufriere Hills Volcano by degassing-induced crystallization, *Terra Nova*, *12*, 14–20, doi:10.1046/j.1365-3121.2000.00267.x.

Sparks, R. S. J., L. Baker, R. J. Brown, M. Field, J. Schumacher, G. Stripp, and A. L. Walters (2006), Dynamical constraints on kimberlite volcanism, *J. Volcanol. Geotherm. Res.*, *155*, 18–48, doi:10.1016/j.jvolgeores.2006.02.010.

Tuffen, H., D. Dingwell, and H. Pinkerton (2003), Repeated fracture and healing of silicic magma generates flow banding and earthquakes?, *Geology*, *31*, 1089–1092.

Voight, B., et al. (2006), Unprecedented pressure increase in deep magma reservoirs triggered by lava-dome collapse, *Geophys. Res. Lett.*, *33*, L03312, doi:10.1029/2005GL024870.

Voight, B., et al. (2010), Unique strainmeter observations of Vulcanian explosions, Soufrière Hills Volcano, Montserrat, July 2003, *Geophys. Res. Lett.*, *37*, L00E18, doi:10.1029/2010GL042551.

Wadge, G., G. S. Mattioli, and R. A. Herd (2006), Ground deformation at Soufrière Hills Volcano, Montserrat during 1998–2000 measured by radar interferometry and GPS, *J. Volcanol. Geotherm. Res.*, *152*, 157–173, doi:10.1016/j.jvolgeores.2005.11.007.

Wadge, G., B. Voight, R. S. J. Sparks, P. Cole, and S. Loughlin (2014), An Overview of the Eruption of the Soufrière Hills Volcano from 2000–2010, in *The Eruption of Soufrière Hills Volcano, Montserrat, From 2000 to 2010*, Geol. Soc. Mem., vol. *39*, edited by G. Wadge, R. Robertson, and B. Voight, pp 1–39, doi:10.1144/M39.1, Geol. Soc., London.

Wang, Z. (2000), *Dynamic Versus Static Elastic Properties of Reservoir Rocks*, SEG Geophysics Reprint Series, *19*, 531–539, Tulsa, OK.